OPTIMUM LAMINAR CONVECTION IN AN ANNULUS OF FINNED DOUBLE PIPE HEAT EXCHANGER

Z. Iqbal[1,*], K. S. Syed[2], M. Ishaq[3]
[1] Department of Mathematics, Government Emerson College, Multan 60700, Pakistan.
[2] CASPAM, Bahauddin Zakariya University, Multan 60800, Pakistan.
[3] Department of Computer Science, COMSATS Institute of Information Technology Vehari 61100, Pakistan.
zafariqbal176@hotmail.com

ABSTRACT. Optimum design configurations of a finned double heat exchanger have been investigated for the enhancement of overall performance i.e. minimization of frictional loss in flow direction and maximization of heat transfer coefficient. The longitudinal fins are made up of highly conducting material with triangular cross-section uniformly distributed outside the inner pipe. A steady, laminar, incompressible and fully-developed flow is taken in the finned annulus of a double pipe with constant heat flux as a thermal boundary condition. The governing PDE'S in terms of momentum and energy equations have been numerically solved by finite element method and the optimization has been performed by genetic algorithm. By taking surface flow area goodness factor as the objective function, various optimum configurations have been proposed depending on practical-industrial requirements and compared with those based on the Nusselt number as an objective function. The present optimum design configurations are cost- and weight-efficient with considerable reduction in pressure loss.

Key Words: Optimum Laminar Convection, Surface flow area goodness factor, Numerical Simulation.

1. INTRODUCTION

Numerical methods and optimization techniques are emerging tools of CFD for optimum designing of various equipments used in different fields of applied sciences and engineering. For the developments and investigations of optimum designs of new products used for different purposes in various disciplines of applied and engineering sciences, these numerical techniques have been reduced partially or completely very costly laboratory or physical experiments. Today one can investigate optimum design through numerical simulation of any physical model and then applying the numerical optimization methods with the help of a digital computer without any physical breaking or changing of the design. Since long ago for the enhancement of heat transfer rate in thermal heat exchange systems the extended surfaces usually termed as fins have been used broadly in various industrial/engineering areas of aeronautics, aerodynamics, electronic equipments, chemical, power, and petroleum processing plants, robots, ships, nuclear reactors and etc. Therefore, the investigation of their optimum design is always remained a hot issue for scientists, researchers, engineers and designers of different disciplines that is why an immense study has been done for their analysis and design. Different researchers have been proposed different shapes like longitudinal and straight fins with trapezoidal, triangular or parabolic cross-section, longitudinal wavy fins, circular pin fins (spines), and annular (radial, circular) fins, etc. and their various configurations for a number of thermal systems subjected to different flow conditions. The use of fins provides an advantage of advancing the rate of heat transfer has many disadvantages like need more pumping power, increase the weight and cost of heat exchanging systems. It is natural to be interested in minimizing all these demerits while maximizing their benefit of enhancing rate of heat transfer. Therefore, it is very critical to use the fins prudently. This raises a multi-objective optimization problem for the designers. They try to choose that design which maximizes the heat transfer rate and minimizes the weight, volume and pressure drop in the flow direction. The fin configuration is determined by the number, thickness, height and annular gap. Optimization of fins critically reviewed in [1, 2].

In literature a deep study may be found for different kinds of longitudinally fins augmented internally/externally to single/double pipes. Such types of finned ducts have been optimized either by investigating optimum fin shape (lateral profile) for specified fin configuration [3-4], or by investigating the optimum configurations of a particular fin shape [5-9]. A comprehensive literature review about fins and classification of problems may be found in [2]. Chang and Hu [5], optimized finned tubes with longitudinal thin fins for laminar convection by employing heat transfer coefficient (Nusselt number) as an objective function. They concluded that the highest heat transfer coefficient, which is approximately 20 times of the tube without fins, is obtained by using 22 fins of height being about 80 percent of the tube radius. This optimum number of fins reduces from 22 to 16 for a sufficiently large rate of heat generation. Colle and Maliska [10] performed the optimization of finned double tubes for laminar convection by using the Green's function and determined a relation between the friction factor, the Reynolds number and fin configuration parameters. Fabbri [3] did the heat transfer optimization in finned annular ducts for laminar convection by using finite element method for the computation of velocity and temperature fields. He found the wavy (polynomial profile of higher order) fins best in performance with equivalent diameter as the characteristic length. Zeitoun and Heagazy [6] presented the idea of different fin heights for the enhancement of heat transfer for laminar convection in internally finned pipes with uniform wall temperature. They concluded that for laminar convection in internally finned pipes, the fin height plays significant role. However the heat transfer optimization of finned double pipe is not a long listed work.

Syed [11] studied the effects of fin and double pipe dimensions on the heat and pressure loss for laminar convection in the finned double-pipe (FDP) with longitudinal trapezoidal fins distributed on outside of inner pipe by using finite difference method for the solution of governing system of equations. Then for the same geometry Syed et al. [12] evaluated the performance of FDP in the entrance region of developing flow for various configurations of the finned annulus. Syed et al [13] studied the flow and heat transfer characteristics taking into account the heat transfer coefficient and pressure loss as the measuring parameters by using finite element method for the solution of governing momentum and energy equations. They considered the FDP problem with triangular fins for laminar convection. The authors [11-13] investigated the effect of finned annulus configurations determined by the number of fins, the fin height, the fin thickness and the annular gap, on the Nusselt number, friction factor and pressure loss by taking only finite values of these configurations. In this

work, we have determined optimum configurations of the triangular finned annulus within in their specified ranges. Surface flow area goodness factor has been taken as an objective function. The optimum configurations investigated by the authors [7-9] taking Nusselt number as an objective function have been compared those of the present of objective function.

The work has been presented as: The mathematical model of the problem has been formulated in Section 2. Procedure for finding the numerical solution is given in Section 3. The optimization problem formulation and its solution procedure are given in Section 4. In Section 5, results and discussion are presented together with a comparison of the present work with those of [8]. Finally concluding remarks are given in Section 6.

2. PROBLEM FORMULATION

A steady, laminar, incompressible and fully developed flow has been assumed in the finned annulus of double. The longitudinal fins made up a highly conductive material with triangular cross-section are straight, non-porous and uniformly distributed outside the inner pipe of FDPHE. Fig.1 and Fig. 2 show the cross-section view and numerical solution domain of the present problem respectively. The H1 [14] boundary conditions have been employed in the cross-section of the triangular finned annulus.

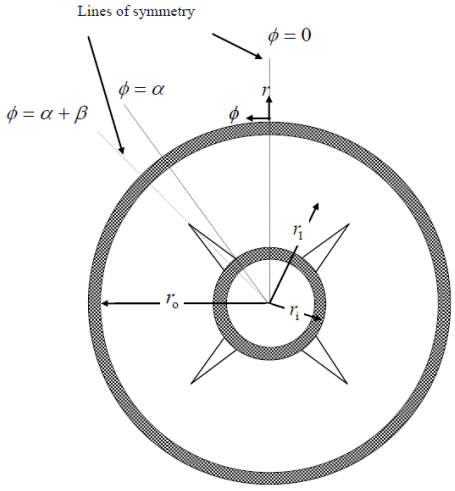

Fig. 1 Cross-section of the finned double pipe

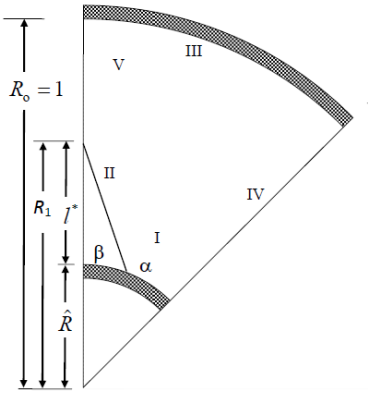

Fig. 2 Numerical domain

2.1. Momentum Equation

The dimensionless form of governing nonlinear momentum equation under the above assumptions of 2-D flow may be written as:

$$\frac{1}{R}\frac{\partial U^*}{\partial R} + \frac{\partial^2 U^*}{\partial R^2} + \frac{1}{R^2}\frac{\partial^2 U^*}{\partial \phi^2} = \frac{-4}{C} \qquad (1)$$

where $C = \left(1 - R_m^2 + 2R_m^2 \ln R_m\right)$ (1a)

and to transform into dimensionless form we have used the following dimensionless variables.

$$U^* = U / U_{max}, R = r / r_o \qquad (2)$$

Here $U_{max} = -(1/4\mu)(dp/dz) r_o^2 \left\{1 - R_m^2 + 2R_m^2 \ln R_m\right\}$ and $R_m = r_m/r_o = \sqrt{1 - \hat{R}^2/2\ln\left(1/\hat{R}\right)}$ with $\hat{R} = r_i/r_o$. The corresponding dimensionless boundary conditions for this geometry are

(a) At the solid boundaries I-III in Fig.2, no-slip conditions ensure that.

(i) $U^* = 0$ at $R = \hat{R}, 0 \le \phi \le \alpha$ (3a)

(ii) $U^* = 0$ at $R = R_1\hat{R}\sin\beta/(\hat{R}\sin(\varphi - \alpha) - R_1\sin(\varphi - \alpha - \beta))$

and $\alpha \le \varphi \le \alpha + \beta$ (3b)

(iii) $U^* = 0$ at $R = 1$ and $0 \le \varphi \le \alpha + \beta$ (3c)

(b) At the lines of symmetry IV-V in Fig.2, the symmetry conditions ensure that

(iv) $\partial U^*/\partial\phi = 0$ at $\varphi = 0$ and $\hat{R} \le R \le 1$ (3d)

(v) $\partial U^*/\partial\phi = 0$ at $\varphi = \alpha + \beta$ and $R_1 \le R \le 1$ (3e)

where $l^* = R_1 - \hat{R}$ is the actual fin height in dimensionless form in Fig. 2.

2.2. ENERGY EQUATION

In dimensionless form the nonlinear energy equation governing the convective heat transfer process under the above assumed flow assumptions may be given as:

$$\frac{\partial^2\theta^*}{\partial R^2} + \frac{1}{R}\frac{\partial\theta^*}{\partial R} + \frac{1}{R^2}\frac{\partial^2\theta^*}{\partial\varphi^2} = \frac{U^*}{A_c^* \overline{U}^*} \qquad (4)$$

where $\theta^*(r) = (\theta(r,z) - \theta_w(z))/(\dot{Q}'/\lambda_f)$ is the temperature filed distribution in dimensionless form, U^* is the velocity distribution in dimensionless form computed from Equation (1) and $\overline{U}^*$ is the average value of U^* over A_c^*, here A_c^* represents the free flow cross-sectional area in dimensionless form.

The computational domain shown in Fig.2 in which the energy equation (4) is to be solved, subject to the following dimensionless boundary conditions.

(a) The boundary conditions of constant heat flux ensure that

(i) $\theta^* = 0$ at $R = \hat{R}$ and $0 \le \varphi \le \alpha$ (5a)

(ii) $\theta^* = 0$ at $R = R_1\hat{R}\sin\beta/(\hat{R}\sin(\varphi - \alpha) - R_1\sin(\varphi - \alpha - \beta))$

and $\alpha \le \varphi \le \alpha + \beta$ (5b)

(b) At the outer pipe an adiabatic wall temperature condition ensures that

(iii) $\partial\theta^*/\partial R = 0$ at $R = 1$ and $0 \le \varphi \le \alpha + \beta$ (5c)

(c) At the lines of symmetry the symmetry conditions ensure that

(iv) $\partial\theta^*/\partial\varphi = 0$ at $\varphi = 0$ and $\hat{R} \le R \le 1$ (5d)

(v) $\partial\theta^*/\partial\varphi = 0$ at $\varphi = \alpha + \beta$ and $R_1 \le R \le 1$ (5e)

3. NUMERICAL SOLUTION

FEM has been employed by using the MATLAB [15] routines for the numerical solution of the governing momentum and energy equations 1 and 4 respectively along-with their corresponding boundary conditions. Adaptive h-refinement has been employed for highly accurate solutions. The FEM formulation and the h-adaptive (George [16]) procedure of this governing system may be found in

[7]. We obtain the velocity and temperature fields by applying the solution procedure of [7] to equations 1 and 4 with the corresponding boundary conditions which are in turn used to evaluate the objective function. In this way every function call from the optimizer invokes the above solution procedure.

4. FORMULATION OF THE OPTIMIZATION PROBLEM AND ITS SOLUTION

For the optimization of a finned double pipe heat exchange systems we always face the issue of appropriate choice of an objective function. If some one's concerned is only to achieve highest transfer rate without concerning the rise in pressure loss, then usually heat transfer coefficient known as *Nusselt* number is considered as an objective function [7-9]. On the other hand, if existing pumping power is restricted and pressure drop is of also anxiety, then it is compulsory to reduce frictional loss maximize rate of heat transfer. This creates a multi-objective optimization problem. However, there is an expression whose optimization involves maximization of heat transfer coefficient (*Nusselt* number) and minimization of frictional loss. This is well-known surface flow area goodness factor widely used as a selection criterion for extended surfaces [17-27]. In the present work we employ this goodness factor as an objective function to find the optimum configuration of the finned annulus of a double pipe with triangular fins attached outside the inner pipe, where configuration is determined by the number of fins, fin height relative to the annular gap, fin thickness and size of the inner pipe relative to the outer pipe. Surface flow area goodness factor is defined as the ratio of Colburn j-factor and Fanning friction f and expressed as [28].

$$j/f = Nu\,\mathrm{Pr}^{-1/3}/(f\,\mathrm{Re}) \qquad (6)$$

Here Nu, Pr and $(f\,\mathrm{Re})$ are respectively *Nuesselt* number, Prandlt number and friction factor in the form of product with Reynolds number.

The surface flow area goodness factor then based on the equivalent diameter averaged over the cross-section may be expressed as.

$$(\overline{j/f})_e = \overline{Nu_e}\,\mathrm{Pr}^{-1/3}/(\overline{f\,\mathrm{Re}})_e. \qquad (7)$$

The average *Nusselt* number $\overline{Nu_e}$ and the average product of Fanning friction factor with Reynolds number $(\overline{f\,\mathrm{Re}})_e$ may be expressed in dimensionless form as [7-9, 11-13 & 3, 5, 7-9].

$$\overline{Nu_e} = D_e^*/(Ph_e^*\theta_b^*) \qquad (8a)$$

$$(\overline{f\,\mathrm{Re}})_e = 2D_e^{*2}/C\overline{U}^*, \qquad (8b)$$

where D_e^* is the equivalent diameter in dimensionless form. θ_b^* is the bulk mean temperature of the fluid in dimensionless form given by

$$\theta_b^* = \iint_{A_c^*} U^*\theta^* dA_c^* \Big/ \iint_{A_c^*} U^* dA_c^* \qquad (8e)$$

C is constant given in equation (1a).

The constraints on the problem parameters M, β, H^* and $\hat{R}$ are the bound constraints determined by the extremes of their ranges considered in the present work which are $M \in \{3{:}3{:}30\}$ $\beta \in [0.5^\circ, 30^\circ]$, $H^* \in [0.05, 0.75]$ and $\hat{R} \in [0.05, 0.75]$, where $H^* = l^*/(1-\hat{R})$.

GA with probabilistic nature has been used as an optimizer. A computer code based on *ga* of global optimization toolbox of MATLAB [15] was developed. The function *ga* employs genetic algorithm. The detailed description and implementation procedure of the optimizer may be found in [7].

5. RESULTS AND DISCUSSION

The numerical solution has been validated by comparing the present results obtained by the FEM with those given in [11] computed by the FDM which is excellent in comparison Table 1. The results have been presented in three subsections. In the first subsection the investigated optimum configurations have presented and discussed. The performance of optimum configurations has evaluated by using various performance measures and selection criteria in the second subsection.

Table 1 Comparison of the present results with the literature results for $H^* = 0.4 : 0.2 : 0.6$, $\beta = 0^\circ$ & $\hat{R} = 0.25$.

H^*	M	$(\overline{j/f})_e$ [11]	$(\overline{j/f})_e$ present
0.4	6	0.4659	0.4656
	12	0.3981	0.3979
	18	0.3547	0.3546
	24	0.3321	0.3322
	30	0.3192	0.3193
0.6	6	0.5993	0.5990
	12	0.4805	0.4798
	18	0.3634	0.3625
	24	0.2981	0.2976
	30	0.2606	0.2603

5.1. OPTIMUM CONFIGURATIONS

In the first step, we investigated optimum configurations of all the four parameters within their ranges which give maximum surface flow area goodness factor (maximum heat transfer rate and minimum frictional loss in the flow direction) by using GA as an optimizer. We denote the optimum values of M, H^*, $\hat{R}$ and β by $M_{opt}, H_{opt}^*, \hat{R}_{opt}$ and β_{opt} respectively. When the surface flow area goodness factor $(\overline{j/f})_e$ defined in Equation 7 is maximized, the overall optimum design configuration are $M_{opt} = 6, H_{opt}^* = 0.75, \beta_{opt} = 0.5$ and $\hat{R}_{opt} = 0.05$ respectively with $(\overline{j/f})_e = 2.7760$.

From these overall optimization results we see that optimum values of the configuration parameters lie at their extreme values considered in the present work. H_{opt}^* lies at its upper extreme value while β_{opt} and $\hat{R}_{opt}$ occur at their smallest values. However, $M_{opt} = 6$ which is not an extreme value in the range of *M*. Thus the optimum fin configuration constitutes, a small number of higher and thinner fins augmented to an inner pipe with very small radius. We also observe that, the hyper-surface of $(\overline{j/f})_e$ varies steadily and smoothly with *M* near its optimum value. This indicates a range of values of *M* around M_{opt} rendering almost the same performance. This leads to the reduction of cost and weight of the finned surface without compromising with the performance if the smallest value of *M* is selected out this range. Since *M* has the highest influence on the performance, cost, weight and volume, therefore, we investigate H_{opt}^*, β_{opt} and $\hat{R}_{opt}$ for specific values of *M*.

Now we present optimization results for specified values of *M* in which H_{opt}^*, $\hat{R}_{opt}$ and β_{opt} have been investigated by maximizing $(\overline{j/f})_e$.

Fig. 3 presents the variation of H^*_{opt}, $\hat{R}_{opt}$, β_{opt} and $(\overline{j/f})_e$ against *M*. We see that H^*_{opt} and β_{opt} lie at their upper and lower bounds respectively for *M* = 3:3:18 and then H^*_{opt} shifts nearer to 0.3 for higher values of *M* while β_{opt} suddenly increases and after attaining its maximum value at *M* = 21 decreases monotonically to 3° for higher values of *M*. The $\hat{R}_{opt}$ always occurs at its lower bound for all values of *M*. Thus for smaller *M*, thinner and longer fins while that for larger *M*, thicker and shorter fins become optimum choice. The values of $(\overline{j/f})_e$ show continuous rise for *M* = 3:3:6, attain their peak value at *M* = 6 and then steadily fall for $M \le 21$. We note that $(\overline{j/f})_e$ does not vary significantly for $21 \le M \le 30$, which provides flexibility in the selection of *M* to meet other needs such as cost, weight and heat load. In analysis of Fig. 5 we may find that for $3 \le M \le 18$, thinner and higher fins will give maximum surface flow area goodness factor while for $M \ge 21$, thicker and shorter fins do so and in both cases the size of the inner pipe is to be as small as possible.

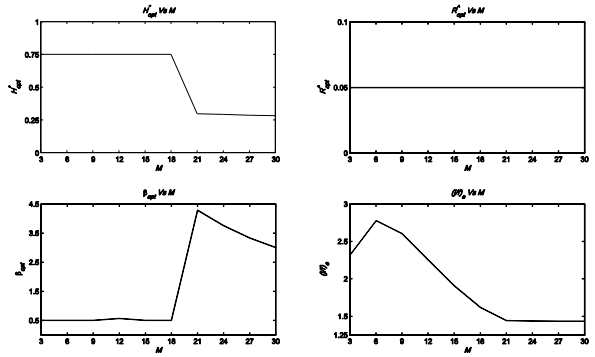

Fig. 3 Optimum design parameters plotted against the number of fins

We noted in the results presented in Fig. 3 $\hat{R}_{opt}$ for the maximization of $(\overline{j/f})_e$ lie at their lowest values and this is true for all values of *M*. These very small values $\hat{R}_{opt}$ may not practically be useful. Therefore, we extend our investigation and find H^*_{opt} and β_{opt} for specified values of $\hat{R}$ and *M*.

Fig. 4 gives the results of $(\overline{j/f})_e$ has been maximized for specified values of $\hat{R}$ and *M*.

We note that for $\hat{R} \le 0.45$, H^*_{opt} occurs at its upper bound for all values of $3 \le M \le 18$ then suddenly falls down towards its lower bound at a certain value of *M* depending on the value of $\hat{R}$. Such ($\hat{R}$, *M*) pairs are (0.05, 21), (0.15, 24), (0.25, 24), (0.35, 27) and (0.45, 30). For $\hat{R} \ge 0.55$, it remains at its upper bound for all number of fins except for the cases of $M = 3$ and $\hat{R} = 0.65, 0.75$ for which it lies at its lower bound. These results show that longer fins will be optimum on larger inner pipes with greater number of fins while shorter fins will be optimum either on larger inner pipes with smaller number of fins or smaller inner pipes with larger number of fins.

β_{opt} occurs at its lower bound for all values of *M* and $\hat{R}$ except for a few cases. It is interesting to note that these exceptional cases for which optimum values of β rises above its lower bound are those for which optimum value of H^* falls down from its upper bound. This behaviour reflects that in the optimum combination of the parameters, higher fins will have to be thinner and thicker fins to be shorter. There is only one exception corresponding to $M = 3$ and $\hat{R} = 0.75$ for which thinner fins are shorter.

From Fig. 4 we also see that the surface flow area goodness factor $(\overline{j/f})_e$ first increases with *M* and after attaining a peak at a certain value of *M* decreases with *M*. The value of *M* at which this peak occurs is larger for larger $\hat{R}$. The $(\overline{j/f})_e$-curve for $\hat{R} = 0.75$ shows steady rise with *M* although not to significant. When we observe the dependence of $(\overline{j/f})_e$ on $\hat{R}$, we note that the smallest inner pipe highly outperforms the inner pipes of larger size for all values of *M*. But this smallest pipe may have least practical value. For $3 \le M \le 21$, $(\overline{j/f})_e$ decreases with $\hat{R}$ while for $21 \le M \le 30$, $(\overline{j/f})_e$ first decreases with $\hat{R}$ but reaching a minimum value starts increasing with further increase in $\hat{R}$. However, variation in $(\overline{j/f})_e$ with $\hat{R}$ is not much significant for larger number of fin($21 \le M \le 30$) as compared to that for $M < 21$. Therefore, for $M \ge 21$, inner pipes of all sizes except $\hat{R} = 0.05$ may be considered to render comparable performance and for this range of number of fins, the size of the inner pipe may be chosen by taking into account other design considerations.

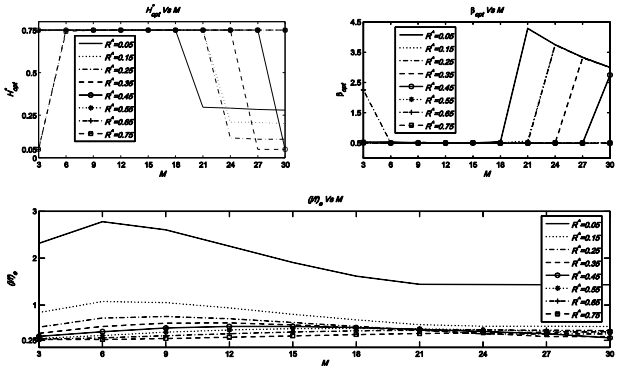

Fig. 4 Optimum design parameters plotted against *M* for specific values of $\hat{R}$

In the present work we have investigated optimum configurations of the finned annulus on the basis of surface flow area goodness factor, $(\overline{j/f})_e$, which takes into account both hydraulic and thermal performance of the optimum configurations. In [8], Z. Iqbal, et al. studied optimum configurations of the finned annulus on the basis of *Nusselt* number which does not take into account their hydraulic performance. It would be interesting for a designer to have a comparison of the thermal and hydraulic performance of the optimum configurations based on both of these objective functions. Table 2 gives % change in the fin volume, friction factor, *Nusselt* number and surface flow area goodness factor of the present optimum configuration relative to those given in [8].

Table 2 shows that by employing the present objective function there is considerable reduction in the pressure loss ranging from 2.80% to 90.16 % accompanied by the reduction in the heat transfer coefficient falling in the range 0% to 86.37%. We note that percentage reduction in $(\overline{f\,\mathrm{Re}})_e$ is larger than that in $\overline{Nu}_e$ for *M* = 3 and $21 \le M \le 30$. The optimum configuration for *M* = 30 gives maximum reduction in $(\overline{f\,\mathrm{Re}})_e$. Moreover, the surface flow area goodness factor being considerably improved by the present objective function with improvement lying in the range 0% to

44.93%, shows maximum gain for the optimum configuration M = 30. Therefore, on the basis of equivalent diameter as a characteristic length, we may say that this optimum configuration is the best one if pressure loss is to be minimized.

The results of fin volume show that for M = 3,15,18 the present optimum configurations are also cost-and weight-efficient in the range 1.69% to 96.86% while for $21 \le M \le 30$ these are less efficient in this regard in the range 126.60% to 232.84%.

Table 2 Percent change in fin volume (V), friction factor, *Nusselt* number and surface flow area goodness factor of the present optimum configuration relative to those given in [8]

M	% change			
	V	$(\overline{f\,\mathrm{Re}})_e$	$\overline{Nu_e}$	$(\overline{j/f})_e$
3	-96.86	-2.80	-0.45	2.41
6	0.00	0.00	0.00	0.00
9	0.00	0.00	0.00	0.00
12	0.00	0.00	0.00	0.00
15	-1.96	0.00	-0.07	0.01
18	-1.69	0.00	0.28	0.01
21	232.84	-86.78	-86.25	3.37
24	190.79	-88.18	-86.37	17.58
27	140.45	-89.34	-85.47	31.59
30	126.60	-90.16	-85.65	44.93

5.2. PERFORMANCE ANALYSIS OF OPTIMUM CONFIGURATIONS

In the present work we have investigated optimum configurations of a finned double pipe rendering maximum surface flow area goodness factor. Although this goodness factor takes into account both the hydraulic and thermal performance, yet it is important to present separately the pressure drop and thermal performance analyses of the optimum configurations of the finned double-pipe relative to the un-finned double-pipe. For the case of specified pumping power, pressure drop in the fully developed region remains constant and is best represented by Fanning friction factor in the form of its product with the Reynolds number. This product has been defined in Eq. (8b).

Thermal performance analysis has been carried out in terms of *Nusselt* numbers in the form its values relative to those for the corresponding un-finned double-pipe. Surface flow area goodness factor has also been presented relative to the corresponding un-finned geometry to evaluate the overall all performance of the finned double pipe relative to the un-finned double pipe.

Fig 5 shows that the relative *Nusselt* number gives rapid increase in comparison to friction factor with *M*. Then after attaining its peak vale at M = 18, it starts decreasing with further increase in *M*. However, it always remains above the friction factor in particular for $3 \le M \le 18$ indicating that gain in heat transfer rate is significantly larger comparison to loss in pressure by using fins. This evaluation is best characterized by the relative surface flow area goodness factor plotted in Fig. 5. We may see from the figure that the relative surface flow area goodness factor is greater than one for all *M* indicating that the optimum configurations of finned surfaces have gain in overall performance over the corresponding finless surfaces. Maximum such gain is around 3 times for the case of M = 6. The results of this figure indicate that if frictional loss is of concern then the optimum range of number of fins may be taken $21 \le M \le 30$ in which maximum deviation of heat transfer coefficient and relative surface flow area goodness factor from their highest values occurring in this range are very small. However, if heat transfer coefficient is of major concern then the optimum range of *M* may be taken to be $12 \le M \le 18$ in which maximum deviation of the relative *Nusselt* number from its largest value is about 7.7%.

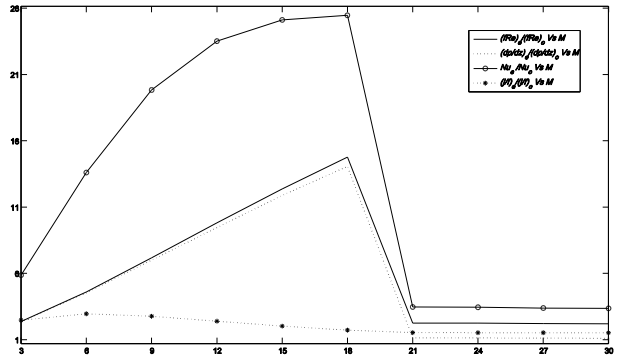

Fig. 5 Relative friction factor, *Nusselt* number and surface flow area goodness factor of optimum configurations plotted against the number.

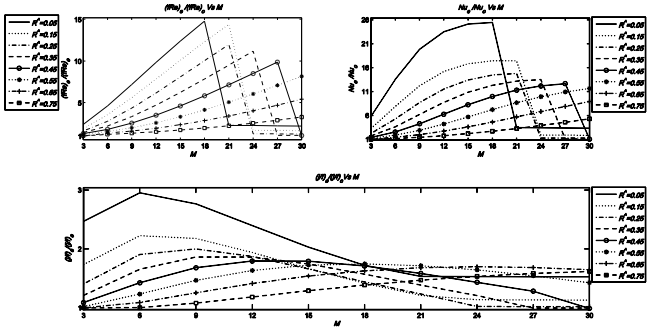

Fig. 6 Relative friction factor, *Nusselt* number and surface flow area goodness factor plotted against the number of fins for specific values of $\hat{R}$.

Fig. 6 shows all the relative measures, for the optimum configurations corresponding to specified values of the ratio of radii and number of fins shown in the figure. We note that the values of relative friction factor and *Nusselt* number vary with *M* in almost a similar fashion for all values of $\hat{R}$. For $0.55 \le \hat{R} \le 0.75$ they increase with *M* while for $0.05 \le \hat{R} \le 0.45$, they have peaks at M = 18, 21, 24 and 27 respectively and having a sudden fall afterward remain constant with further increase in *M*. In the range of *M* where the curves rise, these relative measures decrease with increase in $\hat{R}$. The same is true for the curves, which suffer sudden fall in the range of *M* in which they remain constant. It is interesting to note that in the present case of characteristic length all the relative measures are greater than one. Thus the optimum finned double pipes outperform the corresponding finless ones in terms of heat transfer coefficient as well as flow area goodness factor. The results of relative surface flow area goodness factor suggests the use of a double pipe with $0.05 \le \hat{R} \le 0.35$ for $3 \le M \le 12$ and that with $0.45 \le \hat{R} \le 0.75$ for $M \ge 15$, where $\hat{R}$ and *M* are to be taken in appropriate combinations in view of the figure.

The present results propose a variety of optimum configurations of the finned double pipe that may be employed for optimum use of energy and saving of cost. By choosing the objective function of interest, an optimum configuration may be selected in view of the cost, weight, structural integrity of the wall-fin assembly and the quantity of heat to be transferred.

6. CONCLUSIONS

We have investigated optimum configurations of the triangular finned annulus of a double pipe for highly conducting wall-fin

assembly. The design variables $M, \hat{R}, H^*$ and β have been optimized using surface flow area goodness factor as the objective function to be maximized under laminar flow conditions subjected to constant heat flux per unit length and uniform peripheral temperature boundary conditions. The performance of the investigated optimum configurations has been evaluated by the performance measures based on pressure loss and heat transfer coefficient. This study leads to the following conclusions.

1. In the overall optimization, the optimum configuration of the triangular finned annulus constitutes, six thinner fins with maximum height augmented to an inner pipe of smallest possible radius.
2. When number of fins are specified, for $3 \le M \le 18$, thinner and higher fins will give maximum surface flow area goodness factor while for $M \ge 21$, thicker and shorter fins do so and in both cases the size of the inner pipe is to be as small as possible.
3. When the number of fins and the ratio of radii both are specified, then for $M \ge 21$, inner pipes of all sizes except $\hat{R} = 0.05$ may be considered to render comparable performance and for this range of number of fins, the size of the inner pipe may be chosen by taking into account other design considerations.
4. All the present optimum configurations in comparison to those of [8] give reduction in the pressure loss from 2.80% to 90.16 % accompanied by the reduction in the heat transfer coefficient falling in the range 0% to 86.37%. The percentage reduction in $(\overline{f\,\mathrm{Re}})_e$ is larger than that in $\overline{Nu_e}$ for M = 3 and $21 \le M \le 30$. The optimum configuration for M = 30 gives maximum reduction in $(\overline{f\,\mathrm{Re}})_e$. The surface flow area goodness factor being considerably improved by the present objective function with improvement lying in the range 0% to 44.93%, shows maximum gain for the optimum configuration, of M = 30. Therefore, we may say that this optimum configuration is the best one if pressure loss is to be minimized.
5. For specified number of fins, if frictional loss is of concern then the optimum range of number of fins may be taken $21 \le M \le 30$ in which maximum deviation of heat transfer coefficient and relative surface flow area goodness factor from their highest values are very small. If heat transfer coefficient is of major concern then the optimum range of M may be taken to be $12 \le M \le 18$ in which maximum deviation of the relative *Nusselt* number from its largest value is about 7.7%.
6. For specified values of the ratio of radii and the number of fins, relative surface flow area goodness factor suggests the use of a double pipe with $0.05 \le \hat{R} \le 0.35$ for $3 \le M \le 12$ and that with $0.45 \le \hat{R} \le 0.75$ for $M \ge 15$, where $\hat{R}$ and M are to be taken in appropriate combinations in view of the present results (Fig.6).
7. A designer, by selecting the objective function of interest, may choose an optimum configuration of the finned double pipe from the present results in view of the cost, weight, structural integrity of the wall-fin assembly and the heat duty. The proposed broad spectra of optimum configurations provide an optimum use of energy and handsome saving of cost.

7.

ACKNOWLEDGEMENT

Authors are thankful to the Higher Education Commission (HEC), Government of Pakistan, for its funding under the indigenous 5000 fellowship scheme.

REFERENCES

1. Razelos P. A critical review of extended surface heat transfer. Heat Transfer Eng. 2003; 24(6):11-28.
2. Gosselin L, Gingras T M, Potvin M F. Review of utilization of genetic algorithms in heat transfer problems. Int J Heat Mass Tran 2009; 52:2169-2188.
3. Fabbri G. Heat transfer optimization in finned annular ducts under laminar-flow conditions. Heat Transfer Eng 1998; 19(4):1521-0537.
4. Lan C-H, Cheng C-H, Wu C-Y. Shape Design for Heat Conduction Problems Using Curvilinear Grid Generation, Conjugate Gradient, and Redistribution Methods. Numer Heat Tr A Appl 2001; 39:487-510.
5. Chang YPM, Hu H. Optimization of finned tubes for heat transfer in laminar flow. J Heat Transfer 1973; 95:332-338.
6. Zeitoun O, Hegazy AS. Heat transfer for laminar flow in internally finned pipes with different fin heights and uniform wall temperature. Heat Mass Transfer 2004; 40:253–259.
7. Syed KS, Iqbal Z, Ishaq M. Optimal configuration of finned annulus in a double pipe with fully developed laminar flow. Appl Therm Eng 2011; 31:1435-1446.
8. Iqbal Z, Ishaq M, Syed KS. Optimization of Laminar Convection on the shell-side of Double pipe with triangular fins. Submitted to Arabian J Sci Eng 2011.
9. Iqbal Z, Syed KS, Ishaq M. Optimal convective heat transfer in Double pipe with parabolic fins. Int J Heat Mass Tran 2011; 54:5415–5426.
10. Colle S, Maliska CR. Optimization of finned double tubes for heat transfer in laminar flow. Brazilian Cong. Mech. Eng. Vol. B. (A76-45126 23-31) Rio de Janeiro, Universidade Fedural, 1976; 475-490.
11. Syed KS. Simulation of fluid flow through a double-pipe heat exchanger. Ph.D. Thesis, Department of Mathematics University of Bradford, 1997.
12. Syed KS, Iqbal M, Mir NA. Convective Heat Transfer in the Thermal entrance region of finned double-pipe. Heat Mass Transfer 2007; 43:449-457.
13. Syed KS, Ishaq M, Bakhsh M. Convective heat transfer in the annulus region of triangular finned double-pipe heat exchanger. Comput Fluids 2010; 44:43-55.
14. Shah RK, London AL. Laminar Flow Forced Convection in Ducts. London: Academic Pr; 1978.
15. MATLAB Version 7.13 (R2011b) toolboxes, http://www.mathworks.com/help/techdoc/rn/bs1ef8o.html, 2011.
16. George PL. Automatic Mesh Generation-Application to finite Element Methods. Wiley; 1991.
17. Wolf I, Frankovic B, Vilicic I, Jurkowski R, Bailly A. A Numerical and Experimental Analysis of Heat Transfer in a Wavy Fin-and-Tube Heat Exchanger. Eng Environ 2006; 91-101.
18. Peng H, Ling X, Wu E. An Improved Particle Swarm Algorithm for Optimal Design of Plate-Fin Heat Exchangers. Ind Eng Chem Res 2010; 49:6144–6149.
19. Jang JY, Chen LK. Numerical analysis of heat transfer and fluid flow in a three-dimensional wavy-fin and tube heat exchanger, Int J Heat Mass Tran 1997; 40(16):3981–3990.
20. Yun JY, Lee KS. An Investigation on Heat Transfer Characteristics of Fin and Tube Heat Exchangers using the Geometry Similitude Method. J air-conditioning and refrigeration 1997; 5:57-67.

21. Taler D. Effect of Thermal Contact Resistance on the Heat Transfer in Plate Finned Tube Heat Exchangers. ECI Symposium Series, vol. RP5: Pro. 7th Int. Conf. Heat Exchanger Fouling and Cleaning -Challenges and Opportunities, Editors Hans Müller-Steinhagen, M. Reza Malayeri, and A. Paul Watkinson, Engineering Conf. Int., Tomar, Portugal, July 1 - 6, 2007.
22. Chiou CB, Wang CC, Chang YJ, Lu DC. Experimental Study of Heat Transfer and Flow Friction Characteristics of Automotive Evaporators. ASHRAE Trans 1994; 100(2):575–581.
23. Bharti RP, Sivakumar IP, Chhabra RP. Forced convection heat transfer from an elliptical cylinder to power-law fluids, Int J Heat Mass Tran 2008; 51:1838–1853.
24. Dong J, Chen J, Chen Z, Zhang W, Zhou Y. Heat transfer and pressure drop correlations for the multi-louvered fin compact heat exchangers. Energ Convers Manage 2007; 48:1506–1515.
25. Ndao S, Peles Y, Jensen MK. Multi-objective thermal design optimization and comparative analysis of electronics cooling technologies., Int J Heat Mass Tran 2009; 52:4317–4326.
26. Siddique M, Khaled ARA, Abdul-hafiz NI, Boukhary AY. Recent Advances in Heat Transfer Enhancements: A Review Report. Int J Chem Eng 2010; doi:10.1155/2010/106461.
27. Kuvannarat T, Wang CC, Wongwises S. Effect of fin thickness on the air-side performance of wavy fin-and-tube heat exchangers under dehumidifying conditions. Int J Heat Mass Tran 2006; 49:2587-2596.
28. Shah RK, Sekulić DP. Selection of Heat Exchangers and Their Components, in Fundamentals of Heat Exchanger Design. USA; John Wiley & Sons, Inc Hoboken, NJ; doi: 10.1002/9780470172605.ch10, 2007.

NOMENCLATURE

A	free flow area, m^2
D	diameter, m
dp/dz	pressure gradient in finned geometry, pa/m
f	Fanning friction factor, dimensionless
H^*	fin height relative to the annulus, dimensionless
(j/f)	surface flow area goodness factor, dimensionless
l^*	actual fin height, dimensionless
M	number of fins
Nu	*Nusselt* number, dimensionless
Pr	Prandtl number, dimensionless
Ph	heated perimeter, m
PW	wetted perimeter, m
R	radial coordinate, dimensionless
Re	Reynolds number, dimensionless
$\hat{R}$	ratio of radii of inner and outer pipes, dimensionless
R_1	radial coordinate of the tip of the fin, dimensionless
R_m	radial position of the point of maximum velocity in the annulus without fins, dimensionless
r, ϕ, z	cylindrical coordinates
r_i	outer radius of inner pipe, m
r_m	radial position of the point of maximum velocity, m
r_o	inner radius of outer pipe, m
$\dot{Q}'$	heat transfer rate per unit axial length of the pipe, W/m
U^*	axial velocity component, dimensionless
U_{max}	maximum axial fluid speed at a cross-section, m/s
θ	temperature, °C
α	half-angle between successive fins, rad
β	fin half angle, rad
λ_f	thermal conductivity of the fluid, W/m K

Abbreviations

DP	double pipe
FDP	finned double pipe
FDM	finite difference method
FEM	finite element method
GA	genetic algorithm
V	volume

Subscripts

b	bulk
c	cross-section
e	equivalent diameter
i	inner-pipe
o	outer-pipe
opt	optimum value
w	solid wall

Superscripts

*	dimensionless quantity
$(\bar{})$	over bar, average value